Research Article

Linghui Wang, Zhi Ge, Ning Zhang, Yujie Feng, Yifeng Ling*, and Hongzhi Zhang*

Electrostatic self-assembly effect of Fe_3O_4 nanoparticles on performance of carbon nanotubes in cement-based materials

https://doi.org/10.1515/ntrev-2023-0209
received September 28, 2023; accepted January 26, 2024

Abstract: The beneficial effect of carbon nanotubes (CNTs) to enhance the electrical conductivity and piezoresistivity of cement-based materials was highly contingent upon its dispersion. To achieve an appropriate dispersion of CNTs, ultrasonication, high-speed stirring, and chemical dispersion were commonly used, which raises the risk of structural damage of CNTs caused by the excessive energy. In this study, electrostatic self-assembly of Fe_3O_4 nanoparticles on CNTs was employed to efficiently disperse CNTs. To optimize the dispersion effect of conductive fillers in cement paste, the mix proportions including sodium dodecyl sulfate (SDS) concentration, CNTs concentration, and Fe_3O_4/CNTs ratios were adjusted. The dispersion degree and electrical property were evaluated by UV–vis absorption and zeta potential. In addition, the effect of self-assembled conductive filler dosage on the electrically conductive property of cement pastes was examined. The results show that the occurrence of electrostatic self-assembly was proved by the change of zeta potential, and the grape-bunch structure was observed by transmission electron microscopy. Further, the optimal proportions of self-assembled conductive fillers were 0.20 wt% SDS concentration, 0.05 wt% CNTs concentration, and 1:1 Fe_3O_4/CNTs ratio. The self-assembled conductive filler dosage between 0.02 and 0.10 wt% can effectively improve the electrical conductivity of cement paste with up to 68% reduction of resistivity.

*** Corresponding author: Yifeng Ling,** School of Qilu Transportation, Shandong University, Jinan, 250002, Shandong Province, China, e-mail: yfling@sdu.edu.cn.
*** Corresponding author: Hongzhi Zhang,** School of Qilu Transportation, Shandong University, Jinan, 250002, Shandong Province, China, e-mail: hzzhang@sdu.edu.cn.
Linghui Wang, Ning Zhang: Shandong Hi-speed Group Co. Ltd, Jinan, 250002, Shandong Province, China
Zhi Ge, Yujie Feng: School of Qilu Transportation, Shandong University, Jinan, 250002, Shandong Province, China

Keywords: carbon nanotubes, self-assembled conductive fillers, dispersion, cement paste

1 Introduction

Concrete is widely used in the construction of infrastructure structure, such as highways, bridges, and tunnels. However, concrete structures are susceptible to developing cracks during service life due to brittle material properties and environmental influences, which can potentially result in severe accidents. Consequently, the global community has expressed significant interest in ensuring efficient monitoring and timely maintenance of concrete structures [1–3]. Conventional approaches to monitoring involve the installation of embedded sensors (*e.g.*, strain gauge, optic sensors, piezoelectric ceramic, shape memory alloy, *etc.*) into the concrete structures. However, these traditional sensors have some drawbacks including poor compatibility, high failure probability, short service life, thus making it difficult to achieve a long-term structural monitoring [4,5]. As a solution, the self-sensing cement-based materials have garnered significant attention from researchers owing to their remarkable sensitivity, exceptional durability, and outstanding compatibility with concrete structures [6].

The self-sensing cement-based materials are developed by incorporating nano-conductive fillers into cement materials to achieve performance modification [7,8]. As a functional component, the incorporation of conductive fillers enables the induction of piezoresistivity into ordinary cement-based materials to form new cement-based sensors. The sensitivity of sensors is influenced by many factors, such as filler type, filler content, and filler dispersion [9,10]. Among nano-conductive fillers, carbon nanotubes (CNTs) are found to be able to modify the properties of cement-based materials due to its excellent electrical conductivity, high chemical and thermal stability, and electromagnetic absorption properties [11–13]. In previous studies, the addition of CNTs was observed to induce a

significant decrease in the electrical resistance of cement-based materials [14]. Based on the characteristic of resistance change, many research studies have been done on piezoresistivity and electrical conductivity of CNTs/cement-based materials. Li *et al.* observed that the addition of CNTs produced a remarkable increase in the piezoresistivity of cement pastes, with a fractional change in resistivity up to 14% [13]. Yu *et al.* investigated the piezoresistivity of CNTs/cement-based materials and observed a correlation between the piezoresistive response and compressive stress levels [15]. A study conducted by Han *et al.* demonstrated that the incorporation of CNTs in cement-based materials resulted in a highly responsive and stable behavior under repetitive stress, and further verified a significant response under vehicular loadings [16]. García-Macías *et al.* established a micromechanics model to predict the uniaxial stress-sensing property of CNTs/cement-based materials, which proved to be beneficial for structural health monitoring application [17]. Ding *et al.* reported a new self-sensing cementitious composite using directly growing CNT by *in situ* synthesized method, which was used in a smart system for crack development monitoring with high sensitivity and fidelity, indicating its potential for structural health monitoring [18,19].

Although CNTs/cement-based materials exhibited good piezoresistivity, the improvement of electrical conductivity and mechanical properties were affected by the dispersion of CNTs [20–24]. The uneven dispersion of CNT agglomerates would adversely affect the formation of the internal conductive network of the CNTs/cement-based materials, thus weakening their piezoresistivity [25]. It would also cause increased porosity of cement-based materials, resulting in reduction of mechanical properties [26,27]. Many methods, such as ultrasonication, mechanical stirring dispersion, and chemical dispersion methods were used to improve the dispersion of CNTs [28–30]. Although the above methods offered partial assistance in dispersing CNTs, they were accompanied by certain limitations such as extra energy consumption, potential structural damage of CNTs caused by the excessive ultrasonication energy [31–33].

Electrostatic self-assembly is a method in which atoms or molecules spontaneously arrange into an order structure based on the principle of mutual attraction of opposite charge, which is an effective technique for solving the dispersion of nanomaterials [34]. Additionally, electrostatic self-assembled conductive fillers can exhibit excellent electrical conductivity with a cooperative improvement effect, reinforcing the formation of a conductive network [35]. Many research have studied different types of electrostatic self-assembled fillers and found that the piezoresistive properties of smart cementitious composites was enhanced [31]. Due to its semiconductor and magnetic properties, the nano-Fe_3O_4 particles can realize a controllable distribution under the magnetic field assembled with CNTs, which has a great potential in monitoring application of vulnerable locations while avoiding stress concentration caused by external sensors.

However, limited research studies have been reported on the CNTs–Fe_3O_4 electrostatic self-assembled conductive fillers. In this article, a simple and general procedure for the electrostatic self-assembled CNTs–Fe_3O_4 conductive fillers was demonstrated in order to enhance the dispersion efficiency of CNTs, avoiding the traditional methods of energy consumption and damage of CNTs caused by excessive high energy. The microstructure and dispersion degree of the composite conductive fillers were analyzed, and the optimal ratios of the conductive filler were determined. Additionally, the effect of self-assembled conductive fillers on the electrically conductive properties of cement pastes was also addressed using the optimal ratio.

2 Materials and methods

2.1 Materials

The raw materials used in this study included the multi-walled CNTs, Fe_3O_4 nanoparticles, surfactant, deionized water, and cement. The carboxyl (COOH)-functionalized multi-walled CNTs were purchased from Chengdu (China) Organic Chemical Co. Ltd. Referring to previous study, the size range of CNTs that contributed to the achievement of higher mechanical performance was selected, and the properties of CNTs are listed in Table 1 [36]. The Fe_3O_4 nanoparticles are A.R. grade (diameter: 20 nm, purity: 99.5%) and were supplied by Shanghai Macklin

Table 1: Properties of functionalized CNTs

Type	Outer diameter (nm)	Length (μm)	Purity (wt%)	Specific surface area (m^2/g)	–COOH functionalization (%)
CNT	10–30	10–30	>95	>110	1.55

Table 2: SDS parameters

Relative molecular mass	PH	Water (%)	Inorganic salt content (%)
288.4	7.5–9.5	≤3.0	≤7.5

Table 3: Chemical compositions of cement (wt%)

Components	SiO_2	Al_2O_3	Fe_2O_3	CaO	MgO	SO_3	LOI
Cement	21.96	4.73	3.68	65.30	2.59	0.30	0.66

Biochemical Co. Ltd. An anionic, surfactant sodium dodecyl sulfate (SDS, M_w = 288.38 g/mol), contained non-polar hydrophobic groups that facilitate adsorption onto the surface of CNTs, thereby enhancing their dispersion. Its parameters are presented in Table 2. The experimental water was deionized water prepared in laboratory. P O 42.5 Ordinary Portland cement was used in this study and its chemical compositions is given in Table 3. To eliminate the effect of surfactants on cement-based materials, tributyl phosphate was used as a defoaming agent.

2.2 Self-assembled Fe_3O_4 nanoparticles along CNTs

The preparation flowchart of self-assembled conductive fillers is shown in Figure 1. The CNTs with COOH groups was negatively charged in an alkaline environment [37]. CNTs were first treated by anionic surfactant (SDS) to further make the surface negatively charged. The negatively charged CNTs self-assembled on the surface of positively charged Fe_3O_4 nanoparticles by electrostatic adsorption to form grape bunch structure together. Three parameters were adjusted to optimize the electrostatic self-assembly effect, including SDS concentration, CNTs concentration, and Fe_3O_4/CNTs ratios. The mix proportions of self-assembled conductive fillers are presented in Table 4. The concentration of SDS and CNTs was based on the wt% of SDS–CNTs dispersion.

First, SDS were added into 100 mL deionized water and magnetically stirred at 40°C until fully dissolved, and then evenly mixed with CNTs using glass rod for 30 s. The mixed CNTs dispersion was subjected to a 15 min ultrasonication at 650 W. After that, the absorbance of CNTs dispersion was measured to determine the optimal SDS and CNTs concentration. CNTs and Fe_3O_4 nanoparticles with different mass ratios were added into deionized water (100 mL) and ultrasonically stirred for 20 min at 650 W. Finally, the CNTs–Fe_3O_4 dispersion was first ultrasonically stirred for 30 min and then magnetically stirred at 200 rpm for 2 h under 30°C to complete the electrostatic assembly. The optimal mass ratio of CNTs and Fe_3O_4 nanoparticles was then determined by UV–vis absorption test and transmission electron microscopy (TEM).

2.3 Mix proportion and preparation of cement pastes

A total of ten sets of the self-assembled conductive fillers were prepared, with varying dosages (0, 0.02, 0.04, 0.06, 0.08, 0.1, 0.5, 1.0, 1.5, and 2.0 wt% of cement) for each set. A water to cement ratio (w/c) of 0.35 and a dosage of 0.14 wt % (based on cement) defoaming agent was applied across all the mixes. A mix with pure CNTs (0.1 wt% of cement) was added as a reference. The mixing process of cement-based materials incorporating conductive fillers is illustrated in Figure 2. First, the weighed self-assembled conductive fillers and water were combined using a paste stirrer operating at a low speed of 140 ± 5 rpm for 60 s. Second, cement was added to mix with the composites for an additional 120 s at the same speed, followed by a high speed of 285 ± 10 rpm for another 120 s. After stirring, the paste was poured into the oiled molds with dimensions of 50 mm × 50 mm × 50 mm. Four stainless steel gauze electrodes were equally embedded in the specimen all the way down to measure the electrical resistance across the entire cross-section. The steel gauze had a diameter of 1 mm and was at intervals of 4 mm. The specimens were demoulded 24 h after casting and cured for 28 days at the temperature of 20 ± 1°C and relative humidity of 98 ± 2%. It is worth noting that the dispersion of conductive fillers in water could not guarantee the same level of dispersion after adding in cement [26,38]. Park *et al.* [39] found that CNT with a content range of 0.025–0.4 wt% could uniformly distribute in the matrix when using a stable suspension. Therefore, this article assumed that the dispersion of conductive fillers remained uniformly dispersed after adding in cement.

2.4 Testing methods

2.4.1 Zeta potential

A Zetasizer Nano ZS nano-particle zeta potential analyzer (Malvern, Britain) was utilized to analyze the zeta potential of CNTs dispersion, Fe_3O_4 nanoparticles dispersion, SDS–CNTs

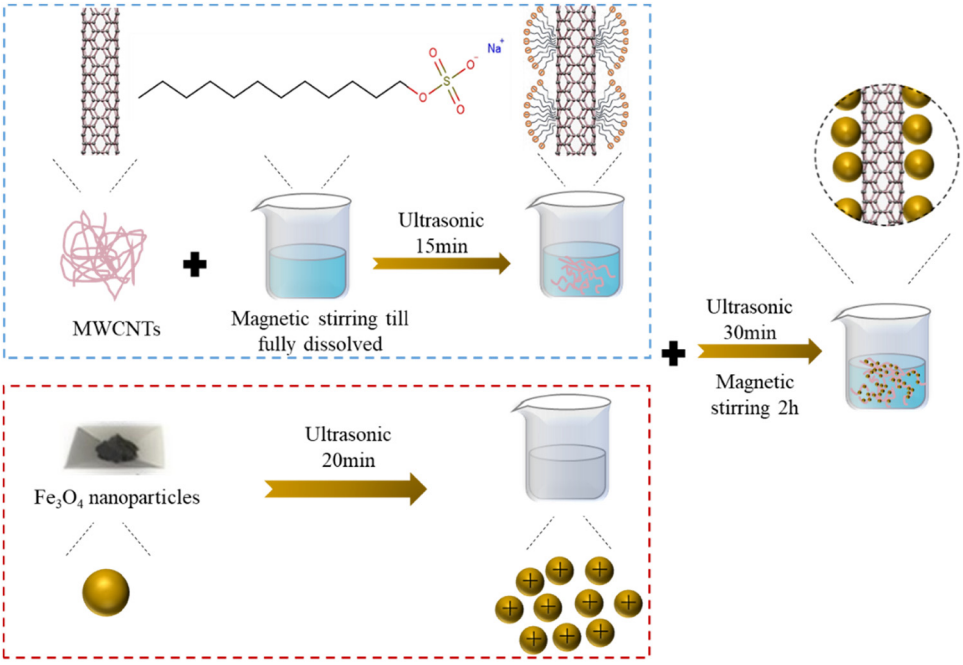

Figure 1: Preparation flowchart of self-assembled conductive fillers.

Table 4: Mix proportions of self-assembled conductive fillers

SDS concentration (wt%)	0.01	0.05	0.1	0.2	0.3	0.4	0.5
CNTs concentration (wt%)	0.01	0.05	0.1	0.5	1.0	1.5	—
Fe_3O_4/CNTs ratio	1:2	1:1.5	1:1	1.5:1	2:1	—	—

dispersion, and CNTs–Fe_3O_4 dispersion. Prior to the test, a small amount of supernatant was taken from the sample using a dropper and the zeta potential was determined after high dilution, with at least three measurements per sample.

2.4.2 UV–vis absorption

Relevant absorption bands corresponding to additional absorption were observed in the UV–vis region for individual CNT particles, while agglomerated CNTs were inactive in the range of wavelength from 200 to 1,100 nm [40,41]. Therefore, a correlation could be established between the quantity of dispersed individual CNT particles and the strength of the absorption spectrum associated with them, and the better the differentiation of the absorption spectrum and the higher absorbance, the better the dispersion of CNTs [42].

The UV–vis absorption spectra were measured using a Metash UV8000 spectrometer in the wavelength range of 200–1,100 nm. In order to achieve a suitable concentration of CNTs for UV–vis measurements, the samples were diluted 100 times by adding a surfactant solution. The concentration of SDS in diluent was similar to that in CNTs dispersion to avoid the colloidal destabilization of CNTs [43]. The blank used was diluted by the same factor, under the same SDS

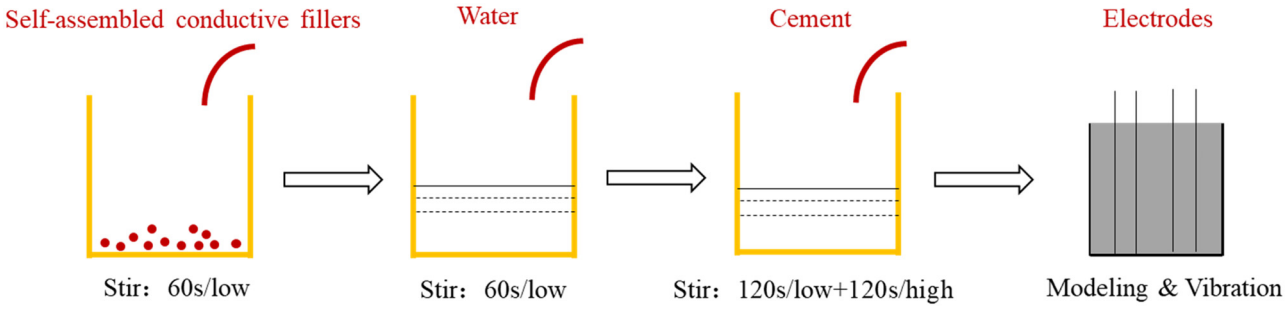

Figure 2: Specimen fabrication process.

concentration as the corresponding sample. For spectrophotometric measurements, three separate preparations and samplings were conducted for each dispersion of CNTs.

2.4.3 Microstructure characterization

A JSM-7610F scanning electron microscopy (SEM) and JEM-1011 TEM were used for microstructure characterization of the electrostatic self-assembled CNTs–Fe_3O_4 conductive fillers. The preparation of the samples involved immersing a copper grid in the CNTs–Fe_3O_4 dispersion, followed by a subsequent drying process.

2.4.4 Electrically conductive measurements

To eliminate the impact of contact resistance, a technique involving four electrodes was employed to measure the potential difference across the specimen [44]. After curing, the specimens were dried at 105°C in oven for 1 day prior to testing. During the measurement, a 305CF direct current (DC) power source was utilized. The voltage and current were observed using a digital multimeter manufactured by Keithley Instruments. The outer two current electrodes were subjected to a constant DC, while the potential difference was measured using the two inner voltage electrodes. The resistance was analyzed in relation to its current flow in order to investigate its ohmic behavior. The resistivity was calculated according $\rho = US/IL$ (where ρ is the resistivity, U is the measured voltage, S is the cross-sectional area, I is the current, and L is the distance between two inner electrodes).

3 Results and discussion

3.1 Characterization of self-assembled conductive fillers

The zeta potential of different conductive filler dispersions is shown in Figure 3. The symbol of the zeta potential represented the electrical properties of ionic surface charges. For solutions with a single electrical property, the greater the absolute value of zeta potential, the better the dispersion stability of the particles in solution [45]. As observed from Figure 3, the surface of Fe_3O_4 particles was positively charged with a potential value of 25.4 mV, while the surface of CNT particles was negatively charged with a potential value of

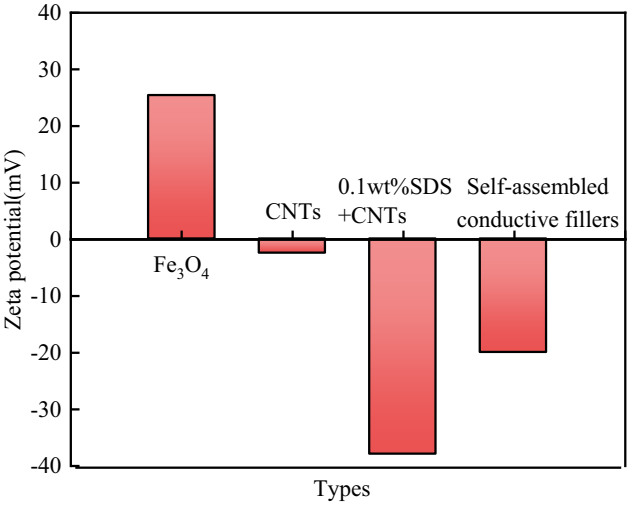

Figure 3: Zeta potential of different dispersions.

−2.5 mV, indicating that CNT particles were poorly stabilized in solution with agglomeration problems [46]. In order to enhance the dispersion of CNTs, 0.1 wt% SDS surfactant was added into the CNTs dispersion. The absolute zeta potential value of SDS–CNTs dispersion was increased to 38.1 mV, illustrating an increased electrostatic repulsion energy between particles and dispersion stability. In addition, the absolute value of zeta potential of 1:1 mixed CNTs–Fe_3O_4 dispersion was reduced to 15.1 mV, which can be attributed to the electrostatic self-assembly of the electrically opposite nanoparticles attracted to each other, resulting in a decrease in the absolute potential value. It is worth noting that the zeta potential of the dispersion after electrostatic self-assembly was not able to analyze its dispersion, which would be further characterized by UV–vis absorption test.

The morphologies of the electrostatic self-assembled CNTs–Fe_3O_4 conductive fillers were further determined by SEM as shown in Figure 4. As can be seen from the figure, there was almost no agglomeration between CNT particles, and a large number of Fe_3O_4 particles were adsorbed on the outer surface of CNTs, which improved the physical contact between CNTs–Fe_3O_4 conductive fillers. The TEM image of the self-assembled CNTs–Fe_3O_4 conductive fillers is given in Figure 5, which showed that the Fe_3O_4 particles were evenly dispersed on the surface of CNTs, forming a synergistic combination effect from grape bunch structure to improve the dispersion of conductive fillers.

It should be emphasized that even after prolonged ultrasonication, the Fe_3O_4 particles could still be tightly immobilized on the CNTs surface, indicating that a robust electrostatic self-assembly occurred between these two types of nanoparticles, preventing their aggregation. At

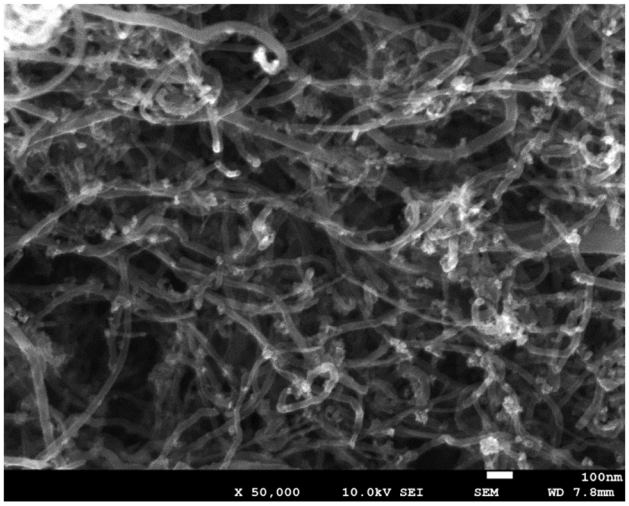

Figure 4: SEM image of self-assembled CNTs–Fe_3O_4 conductive fillers.

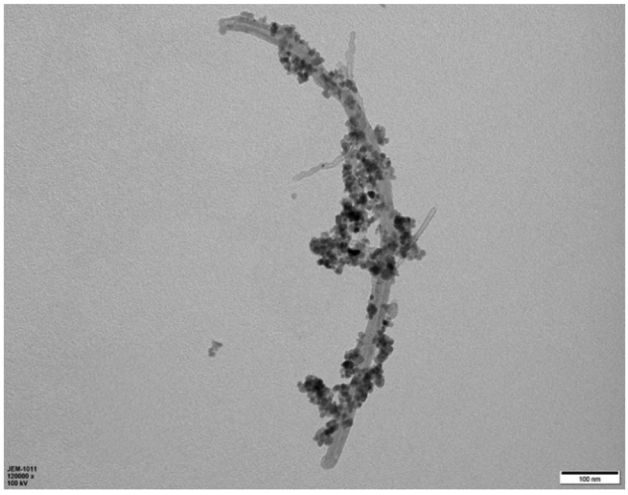

Figure 5: TEM image of self-assembled CNTs–Fe_3O_4 conductive fillers.

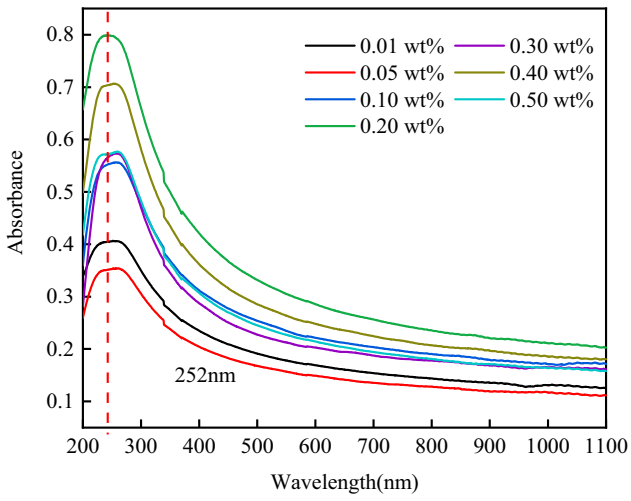

Figure 6: UV–vis absorption spectra of SDS–CNTs dispersions.

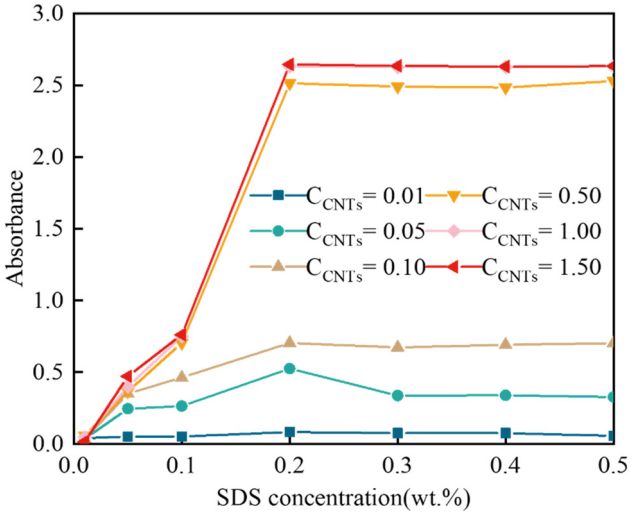

Figure 7: Absorbance of CNTs dispersion.

the same time, Fe_3O_4 particles acted as a spacer between CNT particles, preventing re-stacking to lose specific surface area of CNT particles, consequently enhancing the electrical conductivity of self-sensing cement-based materials.

3.2 Dispersion of self-assembled conductive fillers

3.2.1 Effect of SDS concentration

As shown in Figure 6, seven samples of SDS–CNTs dispersion with different SDS concentrations were selected for UV–vis absorption spectra test. The maximum absorbance of each sample was observed at λ = 252 nm, which was the characteristic absorption wavelength of individual CNT particles. The absorbance of remaining samples was measured at λ = 252 nm.

Figure 7 shows the absorbance of SDS–CNTs dispersion in variation of SDS concentration and CNTs concentration measured at the characteristic wavelength of 252 nm. At the same concentration of CNTs, the absorbance of CNTs dispersion steadily increased as the SDS concentration increased to 0.20 wt% and then slightly decreased when SDS concentration exceeded 0.20 wt%, which corresponded to the dispersion degree of CNTs in the aqueous SDS solutions. For a given SDS concentration, the absorbance of CNTs dispersion gradually increased with the CNTs concentration increasing. When the concentrations of CNTs were 0.01, 0.05, and 0.10 wt%, the absorbance varied significantly with the

SDS concentration, and peaked at 0.08, 0.52, and 0.70, respectively. However, there was little change in absorbance as the concentration of CNTs gradually increased to more than 0.50 wt%. The reason for this phenomenon was mainly related to the critical micelle concentration (cmc), an important property of anionic surfactant to highlight the role of the surfactant state (unimers *vs* micelles) in dispersion [43]. At low concentration, the SDS molecules were less adsorbed on the wall of CNTs, the repulsive force and spatial site resistance between particles were not enough to overcome the agglomeration between CNT particles. When the concentration of SDS was larger than cmc which exceeded the saturated adsorption of SDS on CNTs. Excessive SDS molecules combined in dispersion to generate a large number of micelles, which created osmotic pressure leading to the re-agglomeration of CNT particles [47–49]. According to the results, it can be concluded that the best CNTs dispersion was achieved at the SDS concentration of 0.2 wt%, so all subsequent experiments were carried out with an SDS concentration of 0.20 wt%.

3.2.2 Effect of CNTs concentration

As shown in Figure 8, the absorbance of CNTs dispersion increased initially and then decreased with the concentration of CNTs increasing. As the CNTs concentration increased to 0.05 wt%, the absorbance reached a peak of 0.55, which indicated that the CNT particles were best dispersed at this concentration. When the CNTs concentration exceeded 1.0 wt%, the absorbance of CNTs reached a plateau, which can be attributed to the high content of CNT particles that led to an obvious agglomeration, reaching the maximum dispersion degree of CNTs in the aqueous SDS solutions [50]. Therefore, a suitable concentration of CNTs should be selected in the preparation of self-assembled conductive fillers. CNTs concentration of 0.05 wt% was chosen to prepare the self-assembled conductive fillers for the following tests.

3.2.3 Effect of the Fe_3O_4/CNTs ratio

Figure 9 shows the absorbance of CNTs–Fe_3O_4 dispersions at different ratios. It can be seen that the absorbance of the dispersions initially positively correlated to Fe_3O_4/CNTs ratios before 1:1, with the absorbance increased from 0.51 to 0.69. When the ratio of Fe_3O_4 to CNTs was over 1:1, the dispersion was basically invariant after slightly decreasing. The reason can be explained that Fe_3O_4 particles were adsorbed on the surface of CNTs due to electrostatic interaction, and their own bulk site resistance reduced the Van der Waals' force between CNT particles to improve the dispersion of CNTs. With the increase of ratio up to 1:1, such effect was dominant. However, excessive Fe_3O_4 particles agglomerated, as the surface of CNTs was saturated for Fe_3O_4 adsorption, leading to a small reduction in CNTs dispersion and the absorbance [51].

Moreover, compared with the SDS–CNTs dispersion, the absorbance of the dispersion with a 0.2 wt% SDS concentration and a 0.05 wt% CNTs concentration was 0.52, while that of the dispersion with a 1:1 Fe_3O_4/CNTs ratio was 0.69, which proved that the self-assembly effect was superior to the surfactant for the dispersion of CNTs.

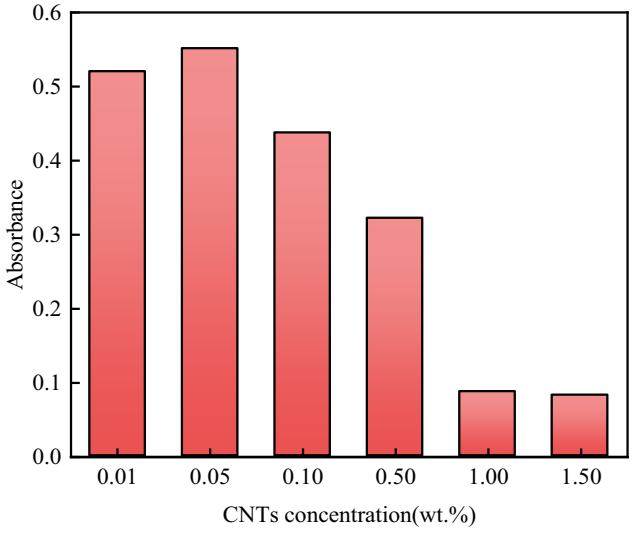

Figure 8: Absorbance of diluted CNTs dispersions.

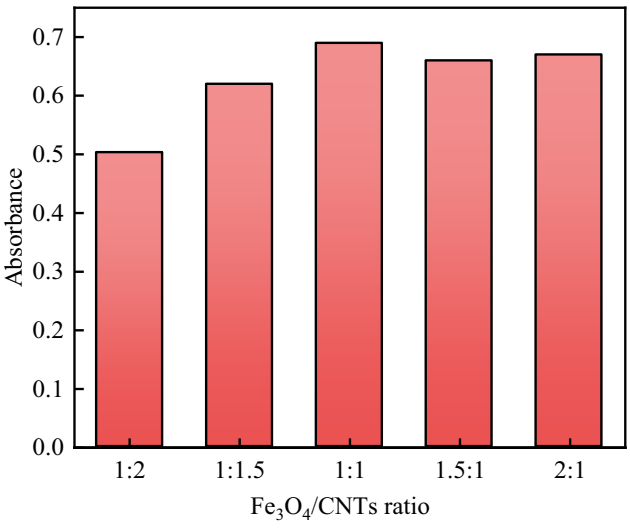

Figure 9: Absorbance of CNTs–Fe_3O_4 dispersions.

3.3 Micro-morphology of self-assembled conductive fillers

Figure 10 shows the morphologies of the self-assembled conductive fillers with different Fe_3O_4/CNTs ratios. With a gradual increase of Fe_3O_4 proportion (1:2–1:1), the amount of Fe_3O_4 particles attached to the CNTs surface increased, forming multiple grape bunch structure, resulting in a better dispersion of CNTs. However, with too many Fe_3O_4 particles (over 1:1), the interparticle attraction was larger than the electrostatic attraction, which made the dispersed CNTs re-agglomerate. The optimal ratio of Fe_3O_4 and CNTs for self-assembled conductive fillers was 1:1.

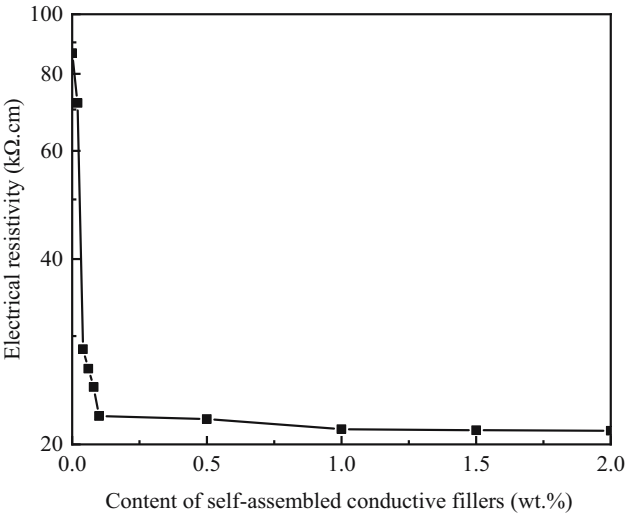

Figure 11: Electrical resistivity of cement pastes with self-assembled conductive fillers.

3.4 Electrically conductive property of cement pastes with self-assembled conductive fillers

Due to the structure of the grape bunches, the conductive fillers can be uniformly dispersed in cement pastes. Based on literature [31], Fe_3O_4 and CNTs played the roles of short-range and long-range conductors in improvement of electrical conductivity for cement pastes, respectively, which was beneficial to piezoresistivity. As illustrated in Figure 11, the electrical resistivity of cement pastes with self-assembled conductive fillers significantly decreased by 68% when the content of self-assembled conductive fillers increased from 0 to 0.1 wt%, indicating that the conductive fillers could form widely distributed conductive network in cement-

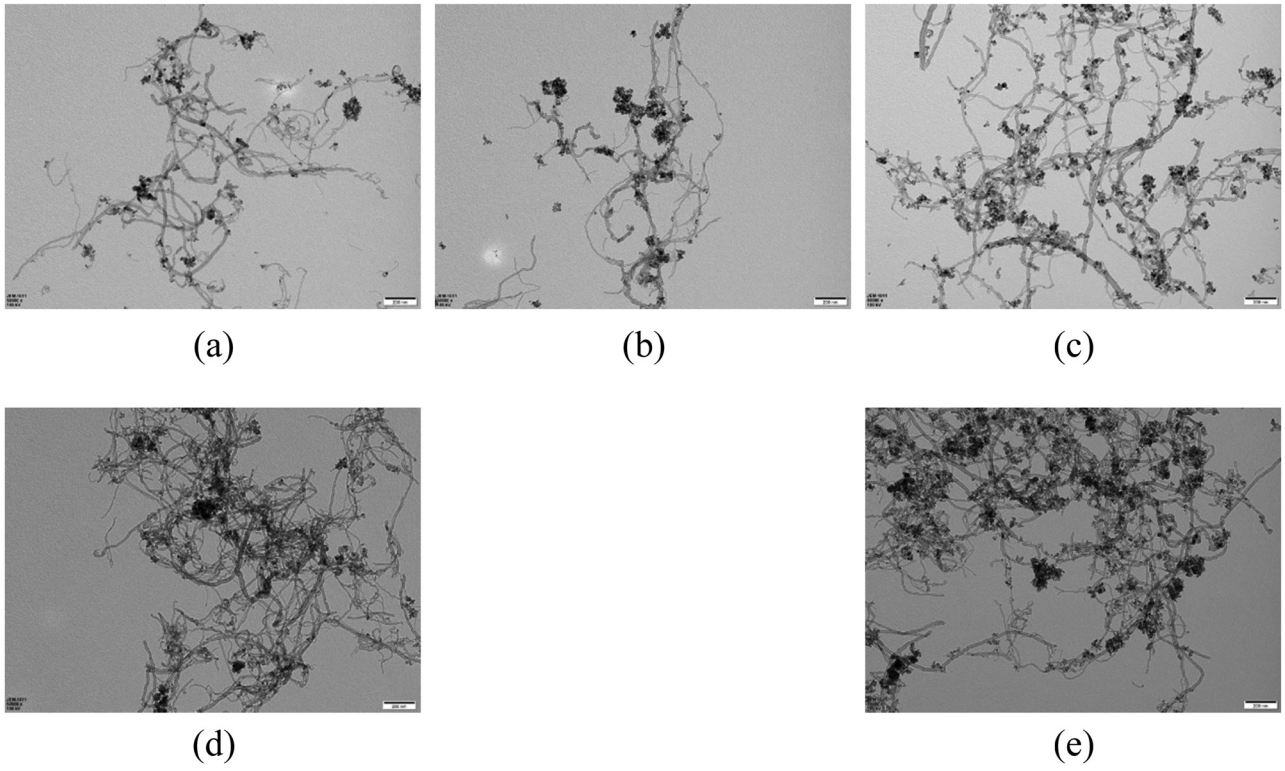

Figure 10: TEM images of self-assembled conductive fillers with different Fe_3O_4/CNTs ratios: (a) 1:2, (b) 1:1.5, (c) 1:1, (d) 1.5:1, and (e) 2:1.

Table 5: Electrical resistivity of cement pastes with different conductive fillers

Conductive filler type	Electrical resistivity (KΩ·cm)
CNTs	26.5
Self-assembled conductive fillers	22.2

based materials. The electrical resistivity of cement-based materials with 0.02–0.1 wt% fillers decreased sharply. However, the resistivity changed marginally later (0.1–2 wt%), representing that self-assembled conductive fillers were excessive to form conductive network. Therefore, the content of conductive fillers between 0.02 and 0.1 wt% was the percolation threshold zone, where piezoresistivity could be displayed [52]. In comparison with results of CNTs–cement-based material (Table 5), the electrical resistivity of cement-based materials with self-assembled conductive fillers was 16.2% lower than that of cement -based materials with CNTs under the same dosage (0.1 wt%), indicating that the self-assembled conductive fillers had a better conductive effect.

4 Conclusions

This article optimized the mix proportions of the electrostatic self-assembled conductive fillers using CNTs and Fe_3O_4 nanoparticles and investigated the effect of CNTs dosage on the electrically conductive property of cement-based materials. The following conclusions were drawn from the experimental results:

1) An easy-to-operate and stable method for the preparation of self-assembled conductive fillers was identified. The zeta potential results indicated that electrostatic self-assembly occurred between two types of nanoparticles, and a grape bunch structure was observed by SEM and TEM.
2) An optimal proportion of self-assembled conductive fillers was developed, *i.e.*, 0.20 wt% SDS concentration, 0.05 wt% CNTs concentration, and 1:1 Fe_3O_4/CNTs ratio.
3) The electrically conductive property of cement-based materials increased with the self-assembled conductive fillers dosage increasing. Compared with the ordinary cement paste, the electrical resistivity was decreased by 68% at a self-assembled conductive fillers dosage of 0.1 wt%.

The ratio optimization of self-assembled conductive fillers improved the efficiency of self-assembly and the dispersion of fillers, and reduced the energy consumption. The increase in electrical conductivity proved that electrostatic self-assembled conductive fillers are promising modification materials to develop multifunctional and smart cement-based composites. The magnetic properties can be further used to carry out related studies.

Funding information: This project was supported by Science and Technology Project of Shandong High Speed Group Co., Ltd (Grant No. 1560021022), the Natural Science Foundation of Shandong Province (Grant No. ZR2021QE174), the Open Project Fund of Key Laboratory of Concrete and Pre-stressed Concrete Structures of Ministry of Education in Southeast University (Grant No. CPCSME2022-03), and the Open Project Fund of Zhejiang Key Laboratory of Civil Engineering Structures & Disaster Prevention and Mitigation Technology (Grant No. ZKLCDF230301).

Author contributions: All authors have accepted responsibility for the entire content of this manuscript and approved its submission.

Conflict of interest: The authors state no conflict of interest.

References

[1] Hang B, Zhang LQ, Ou JP. Smart and multifunctional concrete toward sustainable infrastructures. Berlin: Springer; 2017.
[2] Ubertini F, Laflamme S, Ceylan H, Luigi Materazzi A, Cerni G, Saleem H, et al. Novel nanocomposite technologies for dynamic monitoring of structures: a comparison between cement-based embeddable and soft elastomeric surface sensors. Smart Mater Struct. 2014;23(4):045023.
[3] Galao O, Baeza FJ, Zornoza E, Garcés P. Strain and damage sensing properties on multifunctional cement composites with CNF admixture. Cem Concr Compos. 2014;46:90–8.
[4] Park S, Ahmad S, Yun CB, Roh Y. Multiple crack detection of concrete structures using impedance-based structural health monitoring techniques. Exp Mech. 2006;46(5):609–18.
[5] De Backer H, Corte W, Bogaert P. A case study on strain gauge measurements on large post-tensioned concrete beams of a railway support structure. Insight. 2003;45:822–6.
[6] Dong W, Li W, Tao Z, Wang K. Piezoresistive properties of cement-based sensors: review and perspective. Constr Build Mater. 2019;203:146–63.
[7] Han B, Ding S, Yu X. Intrinsic self-sensing concrete and structures: a review. Measurement. 2015;59:110–28.
[8] Monteiro AO, Loredo A, Costa PMFJ, Oeser M, Cachim PB. A pressure-sensitive carbon black cement composite for traffic monitoring. Constr Build Mater. 2017;154:1079–86.
[9] Han J, Pan J, Cai J, Li X. A review on carbon-based self-sensing cementitious composites. Constr Build Mater. 2020;265:120764.
[10] Bekzhanova Z, Memon SA, Kim JR. Self-sensing cementitious composites: review and perspective. Nanomaterials. 2021;11(9):2355.

[11] Jiang S, Zhou D, Zhang L, Ouyang J, Yu X, Cui X, Han B. Comparison of compressive strength and electrical resistivity of cementitious composites with different nano- and micro-fillers. Arch Civ Mech Eng. 2018;18(1):60–8.
[12] Kang I, Schulz MJ, Kim JH, Shanov V, Shi D. A carbon nanotube strain sensor for structural health monitoring. Smart Mater Struct. 2006;15(3):737–48.
[13] Li GY, Wang PM, Zhao X. Pressure-sensitive properties and microstructure of carbon nanotube reinforced cement composites. Cem Concr Compos. 2007;29(5):377–82.
[14] Coppola L, Buoso A, Corazza F. Electrical properties of carbon nanotubes cement composites for monitoring stress conditions in concrete structures. Appl Mech Mater. 2011;82:118–23.
[15] Yu X, Kwon E. A carbon nanotube/cement composite with piezoresistive properties. Smart Mater Struct. 2009;18(5):055010.
[16] Han B, Yu X, Kwon E. A self-sensing carbon nanotube/cement composite for traffic monitoring. Nanotechnology. 2009;20(44):445501.
[17] García-Macías E, D'Alessandro A, Castro-Triguero R, Pérez-Mira D, Ubertini F. Micromechanics modeling of the uniaxial strain-sensing property of carbon nanotube cement–matrix composites for SHM applications. Compos Struct. 2017;163:195–215.
[18] Ding S, Xiang Y, Ni Y-Q, Thakur VK, Wang X, Han B, Ou J. *In-situ* synthesizing carbon nanotubes on cement to develop self-sensing cementitious composites for smart high-speed rail infrastructures. Nano Today. 2022;43:101438.
[19] Ding S, Wang X, Qiu L, Ni YQ, Dong X, Cui Y, et al. Self-sensing cementitious composites with hierarchical carbon fiber-carbon nanotube composite fillers for crack development monitoring of a Maglev Girder. Small. 2022;19(9):2206258.
[20] Camacho-Ballesta C, Zornoza E, Garcés P. Performance of cement-based sensors with CNT for strain sensing. Adv Cem Res. 2016;28(4):274–84.
[21] Bogas JA, Hawreen A, Olhero S, Ferro AC, Guedes M. Selection of dispersants for stabilization of unfunctionalized carbon nanotubes in high pH aqueous suspensions: application to cementitious matrices. Appl Surf Sci. 2019;463:169–81.
[22] Liew KM, Kai MF, Zhang LW. Carbon nanotube reinforced cementitious composites: an overview. Composites, Part A. 2016;91:301–23.
[23] Mendoza Reales OA, Dias Toledo Filho R. A review on the chemical, mechanical and microstructural characterization of carbon nanotubes-cement based composites. Constr Build Mater. 2017;154:697–710.
[24] Ramezani M. Design and predicting performance of carbon nanotube reinforced cementitious materials: mechanical properties and dispersion characteristics: Electronic Theses and Dissertations; 2019.
[25] Collins F, Lambert J, Duan WH. The influences of admixtures on the dispersion, workability, and strength of carbon nanotube–OPC paste mixtures. Cem Concr Compos. 2012;34(2):201–7.
[26] Ramezani M, Kim YH, Sun Z. Probabilistic model for flexural strength of carbon nanotube reinforced cement-based materials. Compos Struct. 2020;253:112748.
[27] Ramezani M, Dehghani A, Sherif MM. Carbon nanotube reinforced cementitious composites: a comprehensive review. Constr Build Mater. 2022;315:125100.
[28] Zou B, Chen SJ, Korayem AH, Collins F, Wang CM, Duan WH. Effect of ultrasonication energy on engineering properties of carbon nanotube reinforced cement pastes. Carbon. 2015;85:212–20.
[29] Banerjee S, Hemraj-Benny T, Wong SS. Covalent surface chemistry of single-walled carbon nanotubes. Adv Mater. 2005;17(1):17–29.
[30] Sindu BS, Sasmal S. Properties of carbon nanotube reinforced cement composite synthesized using different types of surfactants. Constr Build Mater. 2017;155:389–99.
[31] Zhang L, Zheng Q, Dong X, Yu X, Wang Y, Han B. Tailoring sensing properties of smart cementitious composites based on excluded volume theory and electrostatic self-assembly. Constr Build Mater. 2020;256:119452.
[32] Ramezani M, Kim YH, Sun Z. Modeling the mechanical properties of cementitious materials containing CNTs. Cem Concr Compos. 2019;104:103347.
[33] Ramezani M, Kim YH, Sun Z, Sherif MM. Influence of carbon nanotubes on properties of cement mortars subjected to alkali-silica reaction. Cem Concr Compos. 2022;131:104596.
[34] Chen Y, Xu J, Liu X, Tang Y, Lu T. Electrostatic self-assembly of platinum nanochains on carbon nanotubes: a highly active electrocatalyst for the oxygen reduction reaction. Appl Catal B: Environ. 2013;140–141:552–8.
[35] Zhang S, Shao Y, Yin G, Lin Y. Carbon nanotubes decorated with Pt nanoparticles via electrostatic self-assembly: a highly active oxygen reduction electrocatalyst. J Mater Chem. 2010;20(14):2826.
[36] Ramezani M, Kim YH, Sun Z. Mechanical properties of carbon-nanotube-reinforced cementitious materials: database and statistical analysis. Mag Concr Res. 2020;72(20):1047–71.
[37] Seo J-W, US Shin. Preparation of positively and negatively charged carbon nanotube-collagen hydrogels with pH sensitive characteristic. J Korean Chem Soc. 2016;60(3):187–93.
[38] Ramezani M, Kim YH, Sun Z. Elastic modulus formulation of cementitious materials incorporating carbon nanotubes: probabilistic approach. Constr Build Mater. 2021;274:122092.
[39] Park J, Jung M, Lee Y-W, Hwang H-Y, Hong S-G, Moon J. Quantified analysis of 2D dispersion of carbon nanotubes in hardened cement composite using confocal Raman microspectroscopy. Cem Concr Res. 2023;166:107102–240.
[40] Saito R, Fujita M, Dresselhaus G, Dresselhaus MS. Electronic structure of chiral graphene tubules. Appl Phys Lett. 1992;60(18):2204–6.
[41] Kataura H, Kumazawa Y, Maniwa Y, Umezu I, Suzuki S, Ohtsuka Y, et al. Optical properties of single-wall carbon nanotubes. Synth Met. 1999;103(1):2555–8.
[42] Jiang L, Gao L, Sun J. Production of aqueous colloidal dispersions of carbon nanotubes. J Colloid Interface Sci. 2003;260(1):89–94.
[43] Dai W, Wang J, Gan X, Wang H, Su X, Xi C. A systematic investigation of dispersion concentration and particle size distribution of multi-wall carbon nanotubes in aqueous solutions of various dispersants. Colloids Surf A: Physicochem Eng Asp. 2020;589:124369.
[44] Sun Z, Nicolosi V, Rickard D, Bergin SD, Aherne D, Coleman JN. Quantitative evaluation of surfactant-stabilized single-walled carbon nanotubes: dispersion quality and its correlation with zeta potential. J Phys Chem C. 2008;112(29):10692–9.
[45] Hanaor D, Michelazzi M, Leonelli C, Sorrell CC. The effects of carboxylic acids on the aqueous dispersion and electrophoretic deposition of ZrO_2. J Eur Ceram Soc. 2012;32(1):235–44.
[46] Parveen S, Rana S, Fangueiro R. A review on nanomaterial dispersion, microstructure, and mechanical properties of carbon nanotube and nanofiber reinforced cementitious composites. J Nanomaterials. 2013;2013:1–19.

[47] Alexander K, Sheshrao Gajghate S, Shankar Katarkar A, Majumder A, Bhaumik S. Role of nanomaterials and surfactants for the preparation of graphene nanofluid: a review. Mater Today: Proc. 2021;44:1136–43.
[48] Jiang Y, Song H, Xu R. Research on the dispersion of carbon nanotubes by ultrasonic oscillation, surfactant and centrifugation respectively and fiscal policies for its industrial development. Ultrason Sonochem. 2018;48:30–8.
[49] Islam MF, Rojas E, Bergey DM, Johnson AT, Yodh AG. High weight fraction surfactant solubilization of single-wall carbon nanotubes in water. Nano Lett. 2003;3(2):269–73.
[50] Yu J, Grossiord N, Koning CE, Loos J. Controlling the dispersion of multi-wall carbon nanotubes in aqueous surfactant solution. Carbon. 2007;45(3):618–23.
[51] Chen Y, Yang Q, Huang Y, Liao X, Niu Y. Synergistic effect of multiwalled carbon nanotubes and carbon black on rheological behaviors and electrical conductivity of hybrid polypropylene nanocomposites. Polym Compos. 2018;39(S2):E723–32.
[52] Han B, Zhang L, Sun S, Yu X, Dong X, Wu T, Ou J. Electrostatic self-assembled carbon nanotube/nano carbon black composite fillers reinforced cement-based materials with multifunctionality. Composites, Part A. 2015;79:103–15.